

## Beyond the thermal plume paradigm

C. G. Farnetani<sup>1</sup> and H. Samuel<sup>2</sup>

Received 5 January 2005; revised 18 February 2005; accepted 15 March 2005; published 14 April 2005.

[1] Geodynamic models of thermo-chemical plumes rising in a mantle wind suggest that we should abandon some paradigms based on the dynamics of purely thermal axisymmetric plumes. The head-tail structure is possible but not unique and the lack of a plume head does not preclude a deep origin. Our results suggest that the surface expression of some thermo-chemical plumes may be a headless, age-progressive volcanic chain. Plume tails are laterally heterogeneous, rather than concentrically zoned, because deep heterogeneities are sheared into distinct and long-lasting filaments that will be successively sampled by different volcanoes, as the oceanic plate moves over the plume tail. Finally, calculated S-wave velocity anomalies are consistent with recent plume tomographic images, showing that compositional heterogeneities in the lowermost mantle favour the coexistence of a great variety of plume shapes and sizes. **Citation:** Farnetani, C. G., and H. Samuel (2005), Beyond the thermal plume paradigm, *Geophys. Res. Lett.*, 32, L07311, doi:10.1029/2005GL022360.

### 1. Introduction

[2] The classical mantle plume initiation model provides a framework to interpret intraplate volcanism, whereby continental flood basalts and oceanic plateaus represent partial melting of large plume heads, while the subsequent volcanic tracks represent the continuing magmatism associated with the plume conduit or 'tail' [Richards *et al.*, 1989]. The paradigm of a head-tail structure was recently used as a criterion to establish whether a hotspot is generated by a mantle plume: if hotspot volcanism does not start with a large igneous province, then a deep plume origin is ruled out [Courtilot *et al.*, 2003]. However, from a fluid dynamics perspective, constraining the plume origin cannot be done independently from an understanding of the underlying mantle structure and dynamics. This is particularly true for the Central Pacific where striking observations indicate a heterogeneous lower mantle: (i) broad negative velocity anomalies [e.g., Mégnin and Romanowicz, 2000], (ii) the anticorrelation between shear wave velocity anomalies and bulk sound speed anomalies in the lowermost mantle suggests a chemical rather than a purely thermal origin [Masters *et al.*, 2000], (iii) the astounding isotopic variability observed even in a single volcanic group [Staudigel *et al.*, 1991], (iv) isotopic similarities between recent Polynesian volcanism and the Cretaceous Darwin Rise indicate that heterogeneities may be long lived, leading Janney and Castillo [1999] to infer the failure of the classical plume

model. So, here we are, with a tremendous discrepancy between the widely accepted plume model, basically a mushroom, and the complex shapes and dynamics revealed by geochemistry and by seismology [e.g., Montelli *et al.*, 2004]. The aim of this paper is to bridge the gap between fluid dynamically consistent plume models and the variety of plumes inferred on geophysical grounds. This is important, since much of the continuing debate questioning plume existence is based on very narrow assumptions about what deep mantle plumes should look like. Previous studies have generally considered the dynamics of isolated, purely thermal plumes where an imposed temperature perturbation, or a heated patch, trigger plume initiation. We take a different approach: first, we consider the effect of chemical heterogeneities in the deep mantle, therefore density variations are due to differences in temperature and intrinsic chemical composition [Tackley, 1998; Davaille, 1999; Samuel and Farnetani, 2003]. Second, our plumes rise in a mantle wind induced by an imposed surface 'plate' motion. Third, we consider a compressible mantle. Fourth, we do not apply any ad hoc temperature perturbation, therefore no plume axisymmetry is imposed. Moving beyond the generally accepted assumptions is a fundamental step that allows us to investigate whether paradigms built on purely thermal axisymmetric isolated plume models still hold in a more complex scenario.

### 2. Model

[3] We use the numerical code Stag3D by Paul Tackley for thermo-chemical convection of a compressible viscous fluid solving the continuity equation, conservation of momentum, conservation of energy and conservation of a compositional field, as thoroughly described by Tackley [1998]. Our three dimensional Cartesian domain (x:y:z) has a size of 8670:4335:2890 km and a spatial resolution of 33.8:33.8:22.5 km/cell. To model chemical heterogeneities we advect 20 million active tracers (80 tracers/cell) using a fourth-order Runge-Kutta technique. At each time step the tracers distribution is converted into a compositional field. The relevant nondimensional numbers are the surface Rayleigh number:  $Ra_s = \rho_s g \alpha_s \Delta T_{sa} D^3 / \eta_s \kappa = 1.9 \cdot 10^7$ , the surface dissipation number  $Di_s = \alpha_s g D / C_p = 1.2$ , the buoyancy ratio  $B = \Delta \rho_{ch} / \rho_s \alpha_s \Delta T_{sa}$ , the ratio of the stabilizing excess density due to composition over the destabilizing density reduction due to temperature. We use the following constant values for the superadiabatic temperature drop  $\Delta T_{sa} = 2500$  K, mantle depth  $D = 2890$  km, specific heat  $C_p = 1200$  J kg<sup>-1</sup> K<sup>-1</sup>, thermal diffusivity  $\kappa = 0.8 \cdot 10^{-6}$  m<sup>2</sup> s<sup>-1</sup>,  $g = 10$  m s<sup>-2</sup>, and the following surface values for density  $\rho_s = 3500$  kg m<sup>-3</sup>, thermal expansion coefficient  $\alpha_s = 5 \cdot 10^{-5}$  K<sup>-1</sup>, viscosity  $\eta_s = 7 \cdot 10^{21}$  Pa s. At 670 km depth the endothermic phase transition has a Clapeyron slope  $\gamma_{ph} = -2.5$  MPa K<sup>-1</sup> and a density jump

<sup>1</sup>Institut de Physique du Globe, Paris, France.

<sup>2</sup>Department of Geology and Geophysics, Yale University, New Haven, Connecticut, USA.

$\Delta\rho_{ph} = 8\%$ . Just below the phase transition we find  $\rho_{670} = 4300 \text{ kg m}^{-3}$ ,  $\alpha_{670} = 2.2 \cdot 10^{-5} \text{ K}^{-1}$ ,  $T_{670} = 1840 \text{ K}$ , while at the core mantle boundary (CMB)  $\rho_{CMB} = 5490 \text{ kg m}^{-3}$ ,  $\alpha_{CMB} = 0.85 \cdot 10^{-5} \text{ K}^{-1}$ ,  $T_{CMB} = 3450 \text{ K}$ , in good agreement with commonly estimated values. Finally, mantle viscosity varies with depth ( $\eta_{lm} = 7 \cdot 10^{21} \text{ Pa s}$ ,  $\eta_{lum} = 7 \cdot 10^{20} \text{ Pa s}$ , in the asthenosphere  $\eta_a = 2 \cdot 10^{20} \text{ Pa s}$ ) and with temperature, so that hot material may be two orders of magnitude less viscous than the surrounding mantle. At the surface we simulate a spreading ridge by imposing the velocity  $v_x = 6 \text{ cm/yr}$ , in order to have a left (right) moving oceanic ‘plate’ 5780 km (2890 km) long, elsewhere the velocity boundary conditions are free slip. The initial temperature varies as an error function profile across two thermal boundary layers, one at the top, simulating a progressively aging oceanic lithosphere and one at the bottom of the model domain, elsewhere the mantle has a constant potential temperature of  $1300^\circ\text{C}$ . Finally, to reveal the filament structure (Section 3.2) we advect packs of passive tracers using the archived, fully 3-D velocity field of the convection model. A 3-D velocity interpolation within the model grid allows us to resolve narrow features.

### 3. Results

[4] In this paper we address the following questions: Is it necessary to assign a shallow origin to volcanic chains that lack a massive igneous event at the onset of hotspot activity? Do all thermo-chemical plumes exhibit a concentrically zoned tail? Can we predict a variety of plume shapes and sizes, and how do our predictions compare with slow velocity anomalies imaged in the lower mantle? Our aim is to provide a fluid dynamically consistent framework to interpret (or re-interpret) a variety of observations, while it is beyond the scope of this paper to investigate the effect of systematically varying model parameters. Therefore, we present the results of only one numerical model with initial thickness of the denser basal layer  $h = 200 \text{ km}$  and  $B = 0.1$  (i.e., heterogeneous material is 1% denser than the surrounding mantle).

#### 3.1. Head-Tail: Not a Necessary Condition for a Deep Plume Origin

[5] The complex dynamics of an internally convecting thermo-chemical boundary layer leads to the formation of ‘upwelling regions’ where the deep basal flow is converging. We observe broad thermo-chemical anomalies (Figures 1a and 1e), with an irregular, non-axisymmetric shape, 700–1400 km size, extending 1000 km above the CMB. Two end-member cases are then possible: the formation of a spherical head rapidly rising in the lower mantle (Figure 1b), or the formation of a ‘spout’, similar to a column with a poorly developed head (Figure 1f). The spout samples preferentially the upper part of the thermo-chemical boundary layer, hence it has a reduced excess temperature and rising velocity. The ascent of both plumes is hindered by the phase transition, however in the first case (Figure 1c) a large head (diameter  $\phi = 600 \text{ km}$ ) easily reaches the base of the lithosphere. Its high excess temperature ( $\Delta T_{pl} = 250\text{--}300^\circ\text{C}$ ) would induce extensive partial melting and the formation of a large igneous province. In the second case (Figure 1g) plume material ponds below the phase transition, and only a narrow ‘tail’ ( $\phi = 120\text{--}180 \text{ km}$ ,  $\Delta T_{pl} =$

$100\text{--}150^\circ\text{C}$ ) eventually penetrates in the upper mantle. Both plumes have a long lasting hotspot activity (Figures 1d and 1h are 30 My after the previous figures), however the calculated buoyancy flux  $b$  differs by one order of magnitude: for vigorous plume tails  $b = 10\text{--}12 \text{ Mg/s}$ , while for weak tails  $b < 1 \text{ Mg/s}$ . This compares quite well with the buoyancy flux estimated by Sleep [1990], ranging from  $b = 8.7 \text{ Mg/s}$  for Hawaii to  $b = 0.3\text{--}0.9 \text{ Mg/s}$  for several Pacific hotspots. Thermo-chemical plumes may thus have different surface manifestations: massive flood volcanism followed by a vigorous hotspot activity, or only a weak hotspot activity, inducing an age progressive volcanic chain that does not start with a large igneous province. Our results provide a framework to reconcile contrasting observations in the central Pacific. Several hotspots (Foundation, Macdonald, Pitcairn, Rarotonga, Rurutu, Samoa and Society) have only a volcanic chain, therefore a shallow non-plume origin has been proposed [Clouard and Bonneville, 2001]. However, their geochemical signature is far from typical Depleted MORB Mantle but covers a large range of compositions, up to the most extreme HIMU and EMII end-members of the ocean island data array [Staudigel et al., 1991]. Moreover, Samoa has a high  $^3\text{He}/^4\text{He}$  component, most likely derived from a relatively undegassed mantle source [Farley et al., 1992], and a deep origin is supported by seismic tomography [Montelli et al., 2004]. Our results suggest that Samoa and other South Pacific hotspots may have a deep plume origin. Their thermo-chemical nature and the ‘filter effect’ exerted by the phase transition may be responsible for the formation of tails without heads.

#### 3.2. Filaments in a Laterally Heterogeneous Tail

[6] Another paradigm inferred from the dynamics of axisymmetric plumes generated by a heat point source is that plume tails are concentrically zoned due to the entrainment of surrounding mantle [Hauri et al., 1994], hence the isotopic structure across the plume tail should mimic the concentric temperature structure. We investigate the robustness of this paradigm for the case of thermo-chemical plumes without an imposed axisymmetry, paying attention to the excess temperature of the entrained material. In fact it is not sufficient to establish that surrounding mantle rises due to viscous coupling, the key aspect is to establish whether this material is hot enough to melt, so that it can be sampled by a volcano. Figure 1i shows a horizontal section across the plume tail: only material coming from the deep source region (indicated by colored tracers) has the excess temperature required to melt beneath the lithosphere, while surrounding mantle is not efficiently heated by thermal conduction. Therefore, plumes are excellent sampling probes of the deep lower mantle, not of the whole mantle [Farnetani et al., 2002]. It is also evident that plume tails are laterally heterogeneous, with a highly irregular zonation. Across the plume tail radial variations of the vertical velocity ( $\partial v_z / \partial r$ ) induce a shear stress that readily stretches heterogeneities into long filaments. The coexistence of distinct filaments across the plume tail is shown in Figure 1j. It is important to note that filaments will be successively sampled by different volcanoes as the oceanic plate moves over the plume tail. Ideally, the isotopic fingerprint of a distinct filament could be detected in several volcanoes of different ages. Abouchami et al. [2005] find that lead isotope variations between present Kilauea’s lavas

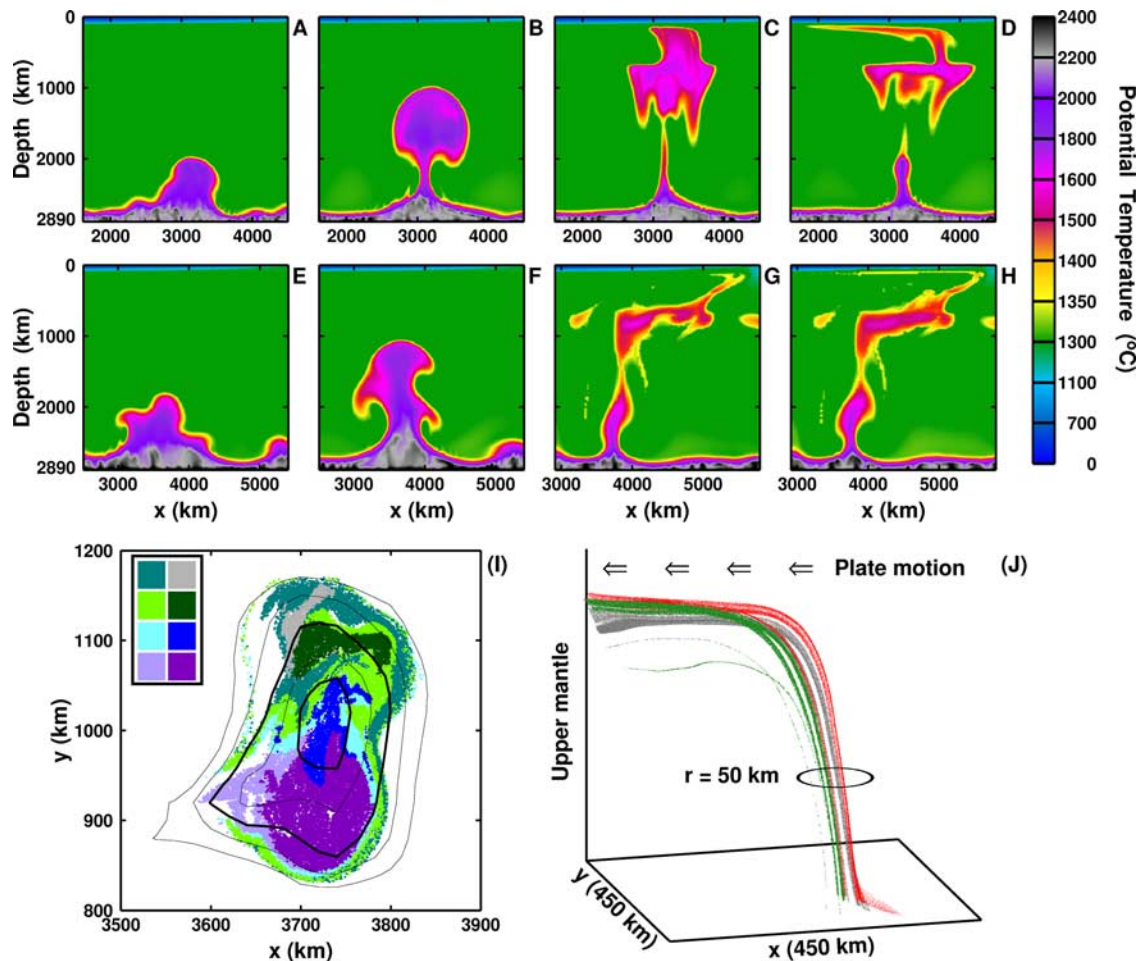


**Figure 1.** Vertical section across three-dimensional plumes. (a) Early stage, (b) formation of a spherical head, (c) large head reaches the lithosphere, (d) 30 My after, the plume is sheared by the left moving oceanic lithosphere. (e) Early stage, (f) formation of a ‘spout’, (g) only a ‘tail’ of plume material reaches the lithosphere, (h) 30 My after. (i) Horizontal section across a plume tail. Excess potential temperature contours each  $50^\circ\text{C}$  (bold  $+100^\circ\text{C}$ ,  $+200^\circ\text{C}$ ). To visualize the material that constitutes the plume tail we advect distinct packs of tracers. The initial pack’s shape (a cube) and dimension (400 km size) are arbitrary, their horizontal position is indicated in the insert, each color corresponds to a pack. The hottest part of the plume tail is made of deep material with a highly irregular, not concentric distribution. (j) Deep mantle heterogeneities rise like distinct filaments in the plume tail and are sheared by left moving oceanic lithosphere.

and Mauna Kea’s lavas over the last 550 ky can be explained by narrow compositional streaks, within the plume tail, that are sampled over time by different volcanoes. This new way of interpreting geochemical variations for Hawaii is in contrast to the commonly accepted concentric zoning model [Hauri *et al.*, 1996] and to the model by Blichert-Toft *et al.* [2003] that neglects the role of shear across the plume tail. Our results strongly indicate that filaments represent a fluid dynamically consistent framework to interpret space and time geochemical variability of hotspot lavas.

### 3.3. A Variety of Shear Wave Velocity Anomalies

[7] Following Samuel *et al.* [2005] we calculate lower mantle shear wave velocity anomalies using the temperature field and the distribution of chemical heterogeneities provided by the dynamical model. Since we consider only  $(\text{Fe}, \text{Mg})\text{SiO}_3$  perovskite and  $(\text{Fe}, \text{Mg})\text{O}$  magnesiowüstite the composition is defined by the silica molar ratio  $x\text{Si} = n\text{Si}/(n\text{Fe} + n\text{Mg})$ , by the iron molar ratio  $x\text{Fe} = n\text{Fe}/(n\text{Fe} +$

$n\text{Mg})$ , and by the iron-magnesium partition coefficient  $K\text{Fe} = (x\text{Fe}/x\text{Mg})_{\text{mw}}/(x\text{Fe}/x\text{Mg})_{\text{pv}} = 3.5$ . We calculate shear wave velocity as a function of pressure, temperature and composition for the pyrolitic reference mantle ( $x\text{Fe} = 0.11$ ,  $x\text{Si} = 0.68$ ) and for the iron enriched ( $x\text{Fe} = 0.15$ ) denser material (see Samuel *et al.* [2005] for a detailed analysis). Velocity anomalies are calculated with respect to the velocity profile of a homogeneous pyrolitic mantle with an adiabatic temperature gradient. Figure 2a shows the coexistence of different types of plumes: a broad dome, more

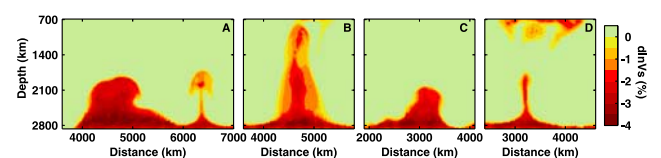


**Figure 2.** (a)–(d) Calculated S-wave velocity anomalies in the lower mantle for a variety of thermo-chemical plumes.



than a thousand kilometers wide, is just next to a narrow mushroom-like plume. Although the coexistence of different plumes has been suggested by *Davaille et al.* [2003] and *Courtillot et al.* [2003], we still lack a thorough understanding of the thermo-chemical boundary layer dynamics leading to the simultaneous generation of strikingly different types of plumes. Thermo-chemical convection provides a way to interpret the complex shear wave velocity structure recently imaged in the lower mantle: Figures 2b and 2c are quite similar to the broad negative velocity anomalies with sharp edges, found by *Romanowicz and Gung* [2002] beneath the South Atlantic and the Pacific, respectively. We note that the ‘spout’ plume (Figure 2b) crossing the whole lower mantle has an average diameter of 500 km but slow ascent velocity ( $v_z = 10\text{--}12$  cm/yr). Finally, we show that shear wave velocity anomalies may be attenuated/absent in the mid mantle due to a severe necking of the plume tail. In Figure 2d negative velocity anomalies are present only beneath the phase transition (due to lateral spreading of the plume) and in the lowermost mantle. In such cases the lack of a continuous velocity anomaly in the lower mantle does not imply a shallow plume origin, but may reflect a discontinuous plume flux.

#### 4. Conclusion

[8] Compositional heterogeneities in the lower mantle play an important role in plume dynamics. Thermo-chemical plumes impinging upon the base of the lithosphere may have a head-tail structure, as expected, or only a tail without head. Therefore, the lack of a plume head does not preclude a deep origin. Our results also show that plume tails are laterally heterogeneous, rather than concentrically zoned. Distinct and long-lasting filaments in the plume tail provide a fluid dynamically consistent framework to interpret space and time geochemical variability of hotspot lavas. Finally, we predict a great variety of plume shapes and sizes, in contrast to the narrow, continuous conduits of classical purely thermal plume models. The consistency of our calculated S-wave velocity anomalies with recent plumes tomographic images strengthens the likelihood of chemical heterogeneities in the deep Earth’s mantle.

[9] **Acknowledgments.** We thank Al Hofmann and Guust Nolet for their constructive and helpful reviews, Claude Jaupart, Anne Davaille and Alexandre Fournier for their encouragement. We are grateful to Paul Tackley for providing the code Stag3D, and to IDRIS (Orsay, France) for supercomputing facilities.

#### References

Abouchami, W., A. W. Hofmann, S. J. G. Galer, F. Frey, J. Eisele, and M. Feigenson (2005), Pb isotopes reveal bilateral asymmetry and vertical continuity in the Hawaiian plume, *Nature*, in press.

- Blichert-Toft, J., D. Weis, C. Maerschalk, A. Agranier, and F. Albaredo (2003), Hawaiian hot spot dynamics as inferred from the Hf and Pb isotope evolution of Mauna Kea volcano, *Geochem. Geophys. Geosyst.*, *4*(2), 8704, doi:10.1029/2002GC000340.
- Clouard, V., and A. Bonneville (2001), How many pacific hotspots are fed by deep-mantle plumes?, *Geology*, *29*, 695–698.
- Courtillot, V. E., A. Davaille, J. Besse, and J. Stock (2003), Three distinct types of hotspots in the Earth’s mantle, *Earth Planet. Sci. Lett.*, *205*, 295–308.
- Davaille, A. (1999), Simultaneous generation of hotspots and superswells by convection in a heterogeneous planetary mantle, *Nature*, *402*, 756–760.
- Davaille, A., M. LeBars, and C. Carbonne (2003), Thermal convection in a heterogeneous mantle, *C. R. Acad. Sci.*, *335*, 141–156.
- Farley, K. A., J. H. Natland, and H. Craig (1992), Binary mixing of enriched and undegassed (primitive?) mantle components (He, Sr, Nd, Pb) in Samoan lavas, *Earth Planet. Sci. Lett.*, *25*, 183–199.
- Farnetani, C. G., B. Legras, and P. J. Tackley (2002), Mixing and deformations in mantle plumes, *Earth Planet. Sci. Lett.*, *196*, 1–15.
- Hauri, E. H., J. A. Whitehead, and S. R. Hart (1994), Fluid dynamic and geochemical aspects of the entrainment in mantle plumes, *J. Geophys. Res.*, *99*, 24,275–24,300.
- Hauri, E. H., J. C. Lassiter, and D. J. DePaolo (1996), Osmium isotope systematics of drilled lavas from Mauna Loa, Hawaii, *J. Geophys. Res.*, *101*, 11,793–11,806.
- Janney, P. E., and P. R. Castillo (1999), Isotope geochemistry of the Darwin Rise seamounts and the nature of long-term mantle dynamics beneath the south central Pacific, *J. Geophys. Res.*, *104*, 10,571–10,589.
- Masters, G., G. Laske, H. Bolton, and A. M. Dziewonski (2000), The relative behavior of shear velocity, bulk sound speed, and compressional velocity in the mantle: Implications for chemical and thermal structure, in *Earth’s Deep Interior: Mineral Physics and Tomography From the Atomic to the Global Scale*, *Geophys. Monogr. Ser.*, vol. 117, edited by S.-I. Karato et al., pp. 63–87, AGU, Washington, D.C.
- Mégnin, C., and B. Romanowicz (2000), The three-dimensional shear velocity structure of the mantle from the inversion of body, surface and higher-mode waveforms, *Geophys. J. Int.*, *143*, 709–728.
- Montelli, R., G. Nolet, F. A. Dahlen, G. Masters, E. R. Engdahl, and S.-H. Hung (2004), Finite-frequency tomography reveals a variety of plumes in the mantle, *Science*, *303*, 338–343.
- Richards, M. A., R. A. Duncan, and V. E. Courtillot (1989), Flood basalts and hotspot tracks: Plumes heads and tails, *Science*, *246*, 103–107.
- Romanowicz, B., and Y. Gung (2002), Superplumes from the core-mantle boundary to the lithosphere: Implications for heat flux, *Science*, *296*, 513–516.
- Samuel, H., and C. G. Farnetani (2003), Thermochemical convection and helium concentrations in mantle plumes, *Earth Planet. Sci. Lett.*, *207*, 39–56.
- Samuel, H., C. G. Farnetani, and D. Andrault (2005), Heterogeneous lowermost mantle: Compositional constraints and seismological observables, in *Structure, Composition and Evolution of Earth’s Mantle*, *Geophys. Monogr. Ser.*, edited by R. D. van der Hilst et al., AGU, Washington, D. C., in press.
- Sleep, N. H. (1990), Hotspot and mantle plumes: Some phenomenology, *J. Geophys. Res.*, *95*, 6715–6736.
- Staudigel, H., et al. (1991), The longevity of the South Pacific isotopic and thermal anomaly, *Earth Planet. Sci. Lett.*, *102*, 24–44.
- Tackley, P. J. (1998), Three-dimensional simulations of mantle convection with a thermo-chemical basal boundary layer: D’’, in *The Core-Mantle Boundary Region*, *Geophys. Monogr. Ser.*, vol. 28, edited by M. Gurnis et al., pp. 231–253, AGU, Washington, D. C.

C. G. Farnetani, Institut de Physique du Globe, 4 pl Jussieu, F-75252 Paris, France. (cinzia@ipgp.jussieu.fr)  
 H. Samuel, Department of Geology and Geophysics, Yale University, New Haven, CT 06520, USA. (henri.samuel@yale.edu)